

Supporting information

Efficient Antibacterial Activity of Hydroxyapatite through ROS

Generation Motivated by Trace Mn(III) Coupled H Vacancy

Ming Wang,^a Miao Li,^a Yunli Wang,^a Yiran Shao,^a Yingchun Zhu^{a, b,*}

a. Key Laboratory of Inorganic Coating Materials CAS, Shanghai Institute of Ceramics Chinese Academy of Sciences, 1295 Dingxi Road, Shanghai 200050, China

b. Center of Materials Science and Optoelectronics Engineering, University of Chinese Academy of Sciences, 19 Yuquan Road, Beijing 100049, China

* Corresponding author, Email: yzhu@mail.sic.ac.cn

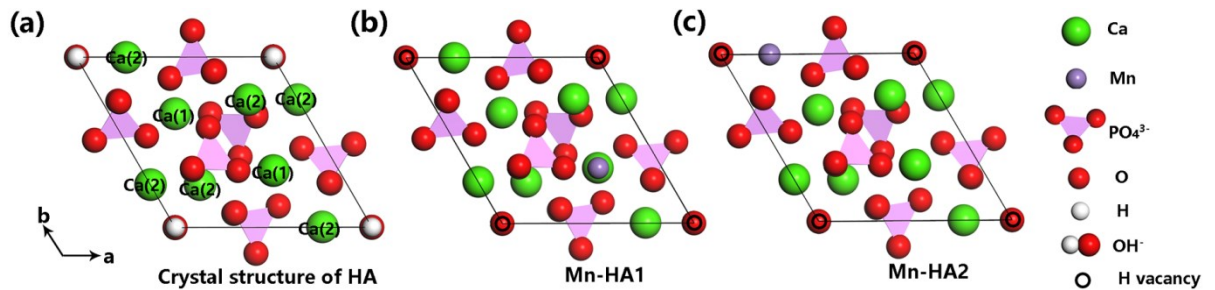


Fig. S1 (a) Presentation of crystal structure of HA. The crystal structure models of Mn^{3+} doped HA [$\text{Ca}_9\text{Mn}(\text{PO}_4)_6(\text{OH})\text{O}$]: (b) Mn-HA1: Mn is substituted at Ca(1) site; (c) Mn-HA2: Mn is substituted at Ca(2) site.

Table S1. The convergence criterion and accuracy of structural optimization process

Convergence criterion	Convergence accuracy
Energy Change (eV/atom)	1.0×10^{-5}
Max. Force (eV/Å)	0.03
Max. Stress (GPa)	0.05
Max. Displacement (Å)	1.0×10^{-3}

Table S2 Primer sequence used for Real-Time PCR

Gene	Primers Sequence	Amplicon Size
GAPDH	Forward: 5'-AGGTCGGTGTGAACGGATTG-3' Reverse: 5'-TGTAGACCATGTAGTTGAGGTCA-3'	123
BMP-2	Forward: 5'- TGGCCCATTAGAGGAGAACCC-3' Reverse: 5'-CTGTGTTCATCTTGGTGCAA-3'	154
Runx2	Forward: 5'-AACGATCTGAGATTGTGGGC-3' Reverse: 5'-CCTGCGTGGGATTCTTGGTT-3'	151

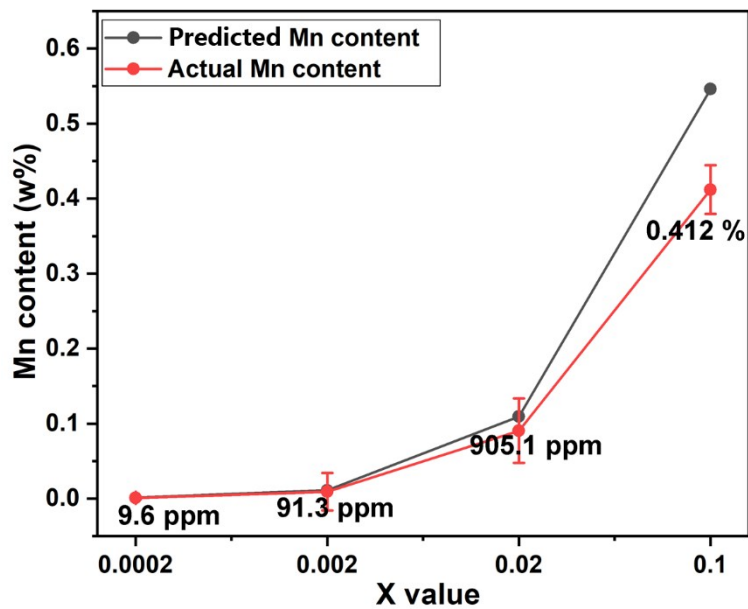


Fig. S2 The Mn contents of Mn-HA.

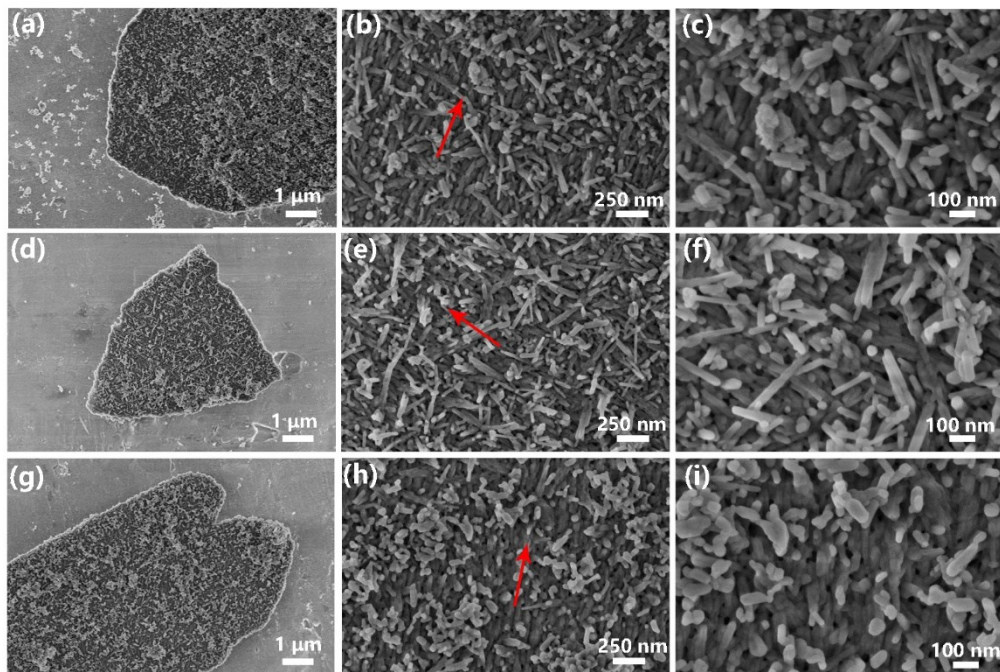


Fig. S3 The SEM images of Mn-HA with different Mn contents. (a-c) HA; (d-f) 0.02Mn-HA; (g-i) 0.1Mn-HA. The red arrow indicated the orientation of assembled nanorods.

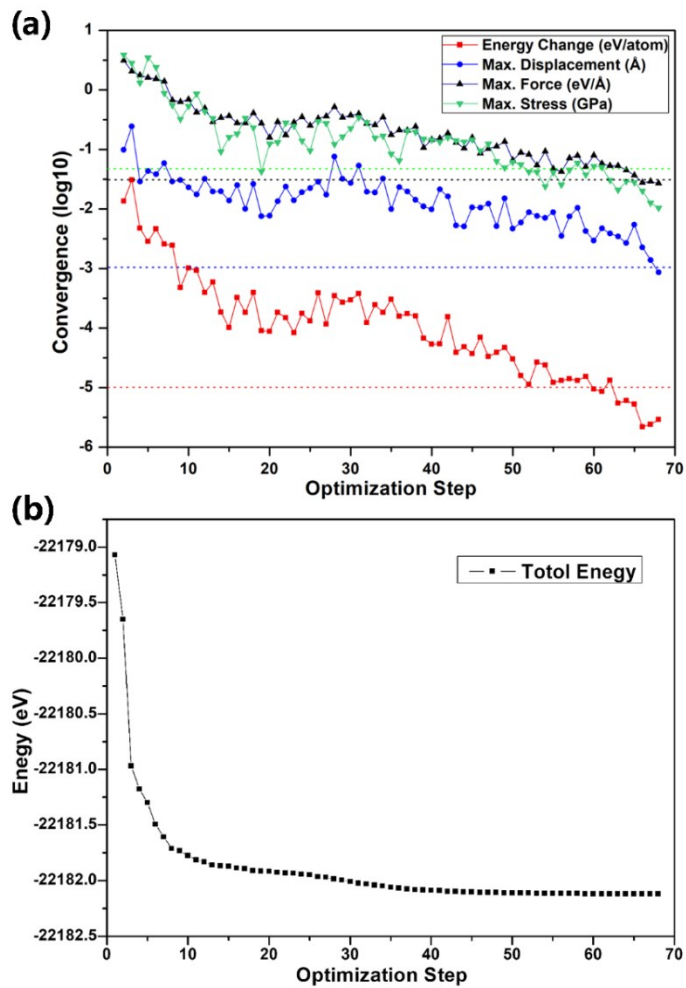


Fig. S4 (a)The convergence curves and (b) Energy value during the calculation process of Mn-HA2.

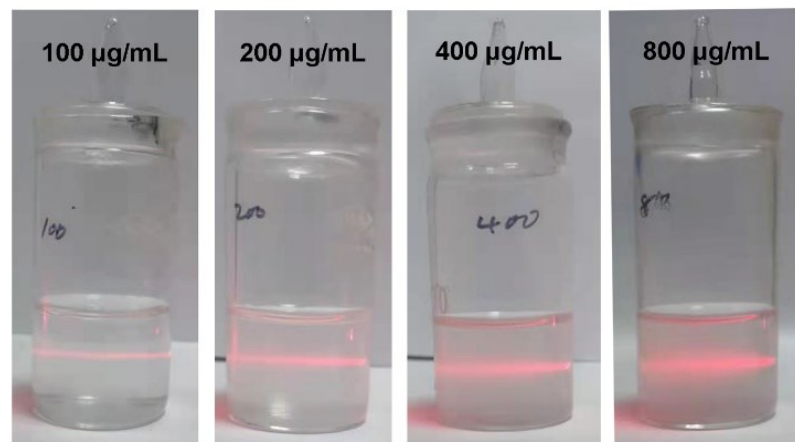


Fig. S5 The colloidal stability of 0.002Mn-HA in PBS.

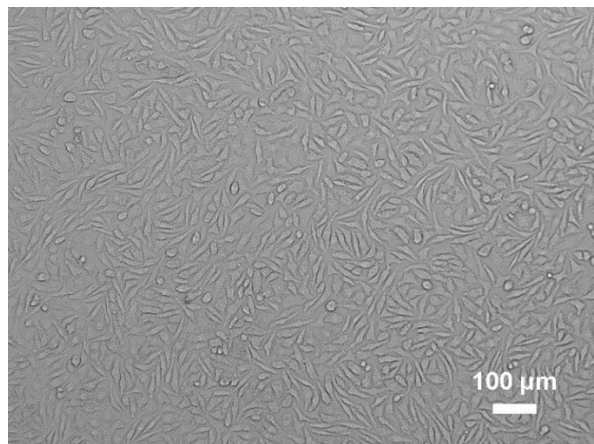


Fig. S6 Morphology image of L929 cells in blank group. The scale bar is 100 μm.